SANS Studies on the Formation of PANI Nanoparticles in the Reverse Micelles

Jae-Hyun Sim, Myungwoong Kim, Sangwook Park, Jeong Hwan Bang,* and Daewon Sohn*

*Department of Chemistry, Hanyang University, Seoul 133-791, Korea. *E-mail: dsohn@hanyang.ac.kr*
**Department of Environmental Health, Seonam University, Namwon 590-711, Korea*
Received July 6, 2005

The formation of polyaniline (PANI) in the reverse micelles of poly(oxyethylene) nonylphenyl ether, (NP5, $H(CH_2)_9Ph(OC_2H_4)_5OH$), was investigated by small-angle neutron scattering (SANS). The reverse micellar solution containing initiators in the inner part of reverse micelle was prepared with surfactant (NP5), water, cyclohexane and an initiator (ammonium persulfate (APS)). The core-shell sphere model containing smearing effect reveals that the polymerization occurs on the shell layer of the reverse micelles. Shell thickness averages varied from 48 Å to 109 Å with increases of monomer concentration.

Key Words : SANS, PANI, Nanoparticles, Micelle, Core-shell

Introduction

Microemulsions are macroscopically homogeneous and optically isotropic colloidal mixtures of two immiscible solvents which are thermodynamically stabilized by amphiphilic molecules.[1-3] Many research groups prepared the conducting polymers such as polyaniline (PANI) and polypyrrole (Ppy) in the micellar structure formed by these amphiphiles, particularly with regards to room temperature preparation.[4,5] In these cases, the monomer and the initiator are placed on the interface of the micelle and the solvent, or inside of the hydrophobic core. Our interest lies in the site of polymerization on the interface between the micelle and the oil phase, formed by non-ionic surfactants such as poly(oxyethylene) nonylphenyl ether (NP5) which does not require co-surfactants.[6]

Though PANI is one of the most promising conducting polymers with many applications, its structural information in solution faced on many difficulties. Absorption spectroscopy simply provides energy state of the PANI particle, but it could not explain the polymerization site in the solution. The structure of the PANI nanoparticle is hardly determined by light scattering because the solution having PANI particles is absorbing the visible radiation. To overcome these difficulties small-angle neutron scattering (SANS) is valuable method for the characterization of the internal structure of micelles or nano-structures containing core and shell parts, especially for the conducting polymers.[7] In this study, the core-shell structure of PANI was determined by the monomer concentration variations and the form factor component of the scattering profiles. We also tried to provide best fitting model for the core-shell structures having polyaniline (PANI) shells in the SANS experiment.

Experimental Section

Samples. Poly(oxyethylene) nonylphenyl ether (NP5, Igepal® CO-520) ($H(CH_2)_9Ph(OC_2H_4)_5$ OH), aniline (99.5%), and ammonium persulfate (APS 99.99–%), and cyclohexane (99+%, purified by distillation) were purchased from Aldrich. Micro-emulsions were prepared by mixing cyclohexane (75 ml) and NP-5 (0.17 M) in a two-necked round bottom flask with mild stirring for 2 h, and then deionized water (deionized at 18 M) with an initiator and the monomer were added. The concentration of each reagent for the polymerization is illustrated in Table 1. The reactions were carried out under N_2 atmosphere at 25 °C for 12 h. When polymerizations were terminated, PANI solution was changed to dark blue color.

Table 1. Sample numbers and the concentrations of each monomer and initiator (APS)

Sample numbers	Monomer concentrations (M)	APS (M)
PANI 1	0.02	0.24
PANI 2	0.03	0.24
PANI 3	0.04	0.24
PANI 4	0.46	0.24

Instrument. SANS measurement were performed with all above samples at the HANARO facility in Daejeon, Korea. In SANS measurements a LN_2 cooled Bi/Be filtered beam of a wavelength $\lambda = 6.8$ Å ($\Delta\lambda/\lambda = 0.12$) is used. The angular distribution of scattered neutrons was recorded using a two-dimensional position sensitive detector (65 × 65 cm^2). All samples were loaded into 2 mm path length quartz cells. The scattering intensity was recorded as a function of the magnitude of scattering vector q ($= 4\pi\sin(\theta/2)/\lambda$, where $\theta/2$ is the scattering angle). The sample to detector distance was set to 3 m and the range of q was about 0.008-0.19 $Å^{-1}$. The raw data was reduced using the standard data reduction software at the HANARO facility.

Data Fitting. In SANS, the total scattering intensity $I(q)$ from a solution of monodispersed particles can be represented by the equation,

$$I(q) = KP(q)S(q) \quad (1)$$

where K is the contrast factor, $P(q)$ is an intra-particle scattering function for a single particle, and $S(q)$ is a

scattering function with inter-particle correlations. The contrast factor directly depends on the particle volume fraction and the differences in the neutron scattering lengths of the components such as the particle and solvent.[8] Equation (1) is pertinent in the case of spherical scattering centers and can be developed to cases of non-spherical scattering objects with an effective structure factor. In dilute solutions (i.e., non-interacting particles), the intra-particle contribution dominates the scattering and the function $S(q)$ approaches unity. Thus, Equation (1) can be simplified to Equation (2),

$$I(q) = NP(q) \tag{2}$$

In this condition, the form factor, $P(q)$, for a simple sphere is proportional to $\Phi^2(qR)$, where

$$\Phi(qR) = \frac{3[\sin(qR) - qR\cos(qR)]}{(qR)^3} \equiv 3\sqrt{\frac{\pi}{2}}\frac{J_{3/2}(qR)}{(qR)^{3/2}} \tag{3}$$

Thus SANS data for spherical shaped particles can be fitted to Eq. (2) containing only the form factor $P(q)$, where

$$I(q) = I(0)\left(\frac{3\sin(qR) - qR\cos(qR)}{q^3R^3}\right)^2 + B \tag{4}$$

qR is a multiplication of the scattering vector magnitude and the radius of the sphere, $J_{3/2}$ is the Bessel function of the order of 3/2 and B is the incoherent background. In this experiment, the core-shell structure containing an ellipsoidal core-shell structure was examined in addition to the hard sphere structure model to fit the SANS data. The intensity pattern, $I(q)$, of the core-shell structure that can be applied to the polymer shell in organic solvent is given by the following equation:

$$I(q) = \frac{A}{V_s}\left[\frac{3V_c(\rho_c - \rho_s)J_1(qR_c)}{qR_c} + \frac{3V_s(\rho_s - \rho_{solv})J_1(qR_s)}{qR_s}\right]^2 + B \tag{5}$$

where $J_1(x) = (\sin x - x\cos x)/x^2$, $V_i = (4\pi/3)r_i^3$; A is a scale factor. The subscripts s, c, and $solv$, refer to the shell, core, and solvent, respectively. Therefore, ρ_c is the scattering length density of the core and R_s is radius of the shell. A polydispersed model is also applied to the hard sphere and core-shell sphere. The form factor of a scattering center in a hard sphere or a core-shell sphere was modified by the normalized probability of a sphere, $f(R)$, from Schulz distribution which depends on two variables $(\bar{R}, z)$.

$$P(Q) = \int_0^\infty f(R)|F(Q,R)|^2 dR \tag{6}$$

$$p \equiv (\langle R^2\rangle - \langle R\rangle^2)^{1/2}/\langle R\rangle = 1/\sqrt{z+1} \tag{7}$$

where $\langle R\rangle$ is average particle radius p is the polydispersity. The details of the polydispersity with the Schulz distribution can be found in elsewhere.[9] Various fitting methods, containing core-shell sphere and ellipsoid form factors, were examined and the fitting parameters are in the references.[10-12] Each SANS spectra was fitted using the IGOR PRO software.

Results and Discussion

The various types of form factor profiles used to fit the SANS data of PANI 2 sample are shown in Figure 1.

Prolated ellipsoid and prolated smeared ellipsoid form factors, known as the core-shell type having an aspect ratio, shows good fitting results in many profiles. However, these form factors reveal unreasonable points among the fitting parameters. When using the ellipsoid type form factor, all radii are scaled from the same center in the modeling stage, which means shell radius parameters should be larger than core radius parameters and similar to the core radius parameters in the prolate ellipsoid model.[9,13] In parameters from a prolated ellipsoid form factor, the minor core radius from the center of the ellipsoid to the surface between shell and core along the minor axis is negative, so it is impossible to fit the data using the prolated ellipsoid form factor.

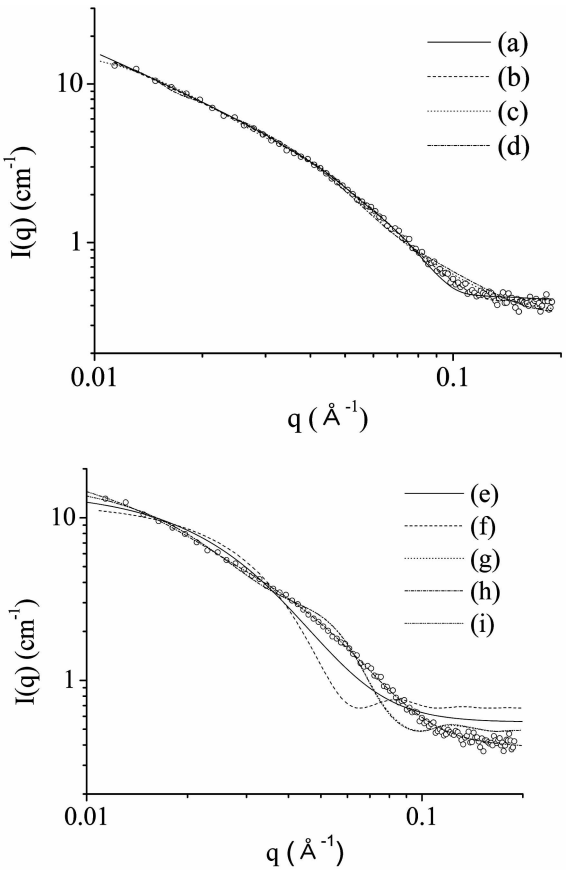

Figure 1. SANS profiles of reverse micelles have PANI 2 and various model fitting profiles from form factors: (a) prolate ellipsoid form, (b) smeared prolate ellipsoid form, (c) oblate ellipsoid form, (d) smeared oblate ellipsoid form, (e) hard sphere form factor, (f) polydispersed hard sphere form factor, (g) smeared core-shell sphere form factor, (h) smeared polydispersed core-shell form factor, and (i) core-shell sphere form factor.

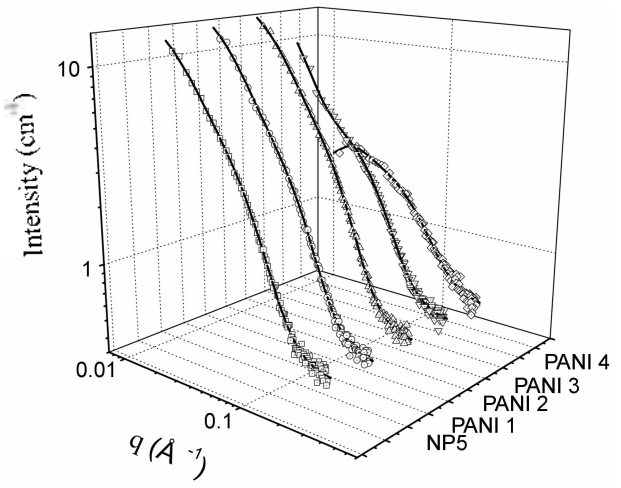

Figure 2. SANS profiles of NP5 reverse micellar sample and PANI sample series: (a) NP5 reverse micellar sample (square), (b) PANI 1 sample (circle), (c) PANI 2 sample (reverse triangle), (d) PANI 3 sample (triangle), (e) PANI 4 sample (diamond). Solid lines are results of the model fitting to experimental data.

Prolated smeared ellipsoid form factor also shows a negative value. Similarly, in the oblate ellipsoid form factor, the fitting result reveals some unpersuasive parameters and smeared oblate ellipsoid form factor are not appropriate models system.[10-12] The best-fit values of each data are obtained by the smeared polydispersed core-shell sphere form factor. The hard sphere, the polydispersed hard sphere, the core-shell sphere, and the smeared core-shell sphere form factor give results in the region, $q > 0.5$; thus, all the SANS data are fitted with the smeared polydispersed core-shell sphere form factor. The result profiles and parameters are shown in Figure 2 and Table 2. In Figure 2, all profiles from polymerization can be compared with a NP-5 reverse micellar solution itself.

In a NP-5 reverse micellar structure, the data of NP-5 reverse micellar solution fits well with smeared core-shell sphere form factor. The fitted result shows that the average diameter from the center of reverse micelle to the surface is about 5.5 nm. When this system is compared to other scattering studies for micelle systems,[14,15] there can be variations in the surface rigidity of micelles and sphere-to-rod transition of micelles in reverse micellar solution due to initiators such as APS.[16-18] In Table 2, fitting results clearly reveal changes of scattering centers as a function of monomer concentration. Because we considered the polydispersity parameter, whole radius information obtained from fitting is an average values. The average shell thickness of sample is plainly increased as monomer concentration is increased. Average core radii show slight irregular changes which occurs in the inner part of reverse micelle with polymer shell during the polymerization. For the NP5 reverse micelle, the average core radii is changed with the deviation of ±3 Å but the average shell thickness of the PANI increased up to 70 Å. PANI 4 sample, which had the highest monomer

Table 2. Fitted parameters for PANI sample series

	PANI 1	PANI 2	PANI 3	PANI 4	NP5 Reverse micelle
Scale (A)	0.394 ± 0.001	0.388 ± 0.001	0.686 ± 0.002	1.296 ± 0.004	0.314 ± 0.005
Average core radius (Å)	16.58 ± 4.28	16.95 ± 3.07	13.48 ± 3.30	11.32 ± 2.57	13.59 ± 3.58
Average shell thickness (Å)	48.52 ± 1.18	47.17 ± 8.32	72.72 ± 1.47	109.71 ± 2.59	39.86 ± 10.5
Overall polydispersity	0.599 ± 0.122	0.592 ± 0.085	0.662 ± 0.115	0.636 ± 0.107	–

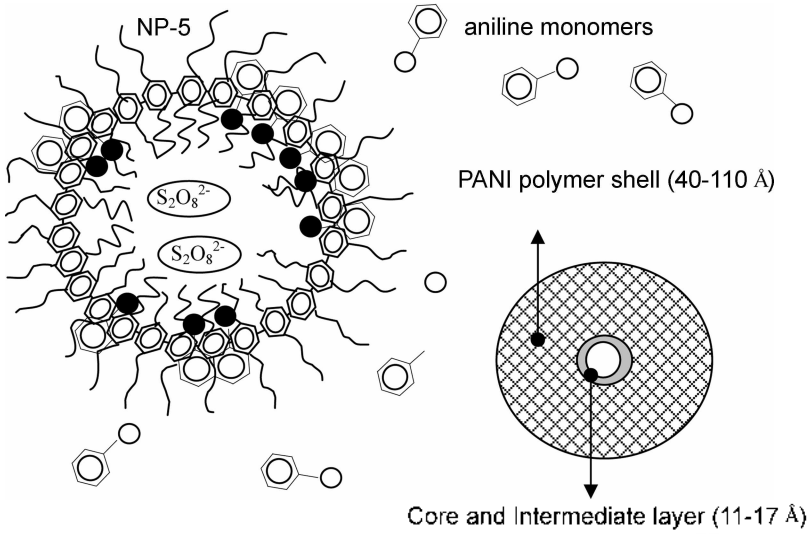

Figure 3. The polymerization process of PANI on reverse micelle surface (○: -NH$_2$ group, ●: -NH$_3^+$ group). Insert (right) shows the core-shell model for the PANI nanoparticle.

concentration, showed a significant increase in average shell thickness owing to the high conversion of PANI itself and a relatively high polymer concentration.[19] Little change of polydispersities of each series in spite of increase of shell thickness means polymerization was gradually and equally progressed on the most scattering centers.[11,20] Scale factors of PANI sample series also become larger as the monomer concentration is increased. The scale factor is proportional to the number density of scattering centers (n), the volume of scattering center (V), and the difference between the particles and the solvent ($\Delta\rho$). Thus, because the reverse micelle concentration is maintained relatively constant, the number density of scattering centers and the difference between the particles and the solvent are maintained constantly during experiments; thus, large values of scale factors of PANI 3 and PANI 4 sample can be accepted as the sudden increase in particle volume. The core radius of each sample is relatively constant and shell thickness increases with increasing monomer concentration, as in the case of the PANI series from 48.5 to 109.7 Å.

Conclusions

Figure 3 shows the schematic diagram of the formation of the PANI nanoparticles. The polymerization occurs shortly after monomer addition and proceeds at the interface between the surfactants and the organic phase. The hard cores formed in the hydrophilic domains inside the micelle and the shell tends to form hydrophobic domains near the core-shell interface. The monomers would be distributed near the shell part of the surfactant and do not penetrate to the core part of the interface. An increase of average shell thickness means not only higher conversion-characteristic onto reverse micelle surface but also easy to control a thickness of shell with change of monomer concentration.

Acknowledgements. Authors greatly acknowledge Dr. Steve Kline of NIST-Gaithersburg, USA for his beneficial advice. D. S. is thankful for the financial support of National R & D Project for Nano Science and Technology in Korea and the ABRL program (grant #: R-14-2002-004-01002-0). This work was supported by KISTEP (grant no. M20202000007-02B0200-00610) for the KAERI for granting beam time at HANARO and the assistance of Mr. B.-S. Sung and Dr. Y.-S. Han.

References

1. Imae, T. *Colloids Surf. A* **1996**, *109*, 291.
2. Sugimoto, T. *Adv. Colloid Interface Sci.* **1987**, *28*, 65.
3. Robinson, B. H.; Kahn-Lodhi, A. N.; Towey, T. *Structure and Reactivity in Reverse Micelles*; Pileni, M. P., Ed.; Elsevier: New York, 1989.
4. (a) Kim, D.; Choi, J.; Kim, J. Y.; Han, Y. K.; Sohn, D. *Macromolecules* **2002**, *35*, 5314. (b) Ryu, K. S.; Kim, K. M.; Hong, Y.-S.; Park, Y. J.; Chang, S. H. *Bull. Korean Chem. Soc.* **2002**, *23*, 1144.
5. Gao, H.; Jiang, T.; Han, B.; Wang, Y.; Du, J.; Liu, Z.; Zhang, J. *Polymer* **2004**, *45*, 3017.
6. Chang, C. L.; Fogler, H. S. *Langmuir* **1997**, *13*, 3295.
7. (a) Hayter, J. B. *Physics of Amphiphiles-Micelles, Vesicles, and Microemulsions*; DeGiorgio, V.; Corti, M., Eds.; Elsevier Science: New York, 1983. (b) Kim, H.-U.; Lim, K.-H. *Bull. Korean Chem. Soc.* **2004**, *25*, 382.
8. Higgins, J. S.; Benoît, H. C. *Polymers and Neutron Scattering*; Clarendon Press: Oxford, 1994.
9. Scalfei, L.; Lanzi, L.; Gambi, C. M. C.; Giordano, R.; Baglioni, P.; Teixeira, J. *J. Phys. Chem. B* **2002**, *106*, 10771.
10. Kotlachyk, M.; Chen, S. H. *J. Chem. Phys.* **1983**, *79*, 2461.
11. Jung, M.; Robinson, B. H.; Steytler, D. C.; German, A. L.; Heenan, R. K. *Langmuir* **2002**, *18*, 2873.
12. Bergström, M.; Pederson, J. S. *J. Phys. Chem. B* **1999**, *103*, 8502.
13. Berr, S. S. *J. Phys. Chem.* **1987**, *91*, 4760.
14. Nakano, M.; Matsuoka, H.; Yamaoka, H.; Poppe, A.; Richter, D. *Macromolecules* **1999**, *32*, 697.
15. Ottewill, R. H.; Rennie, A. R.; Laughlin, R. G.; Bunke, G. M. *Langmuir* **1994**, *10*, 3493.
16. Kumar, S.; Aswal, V. K.; Goyal, P. S.; Din, K. *J. Chem. Soc.* **1998**, *94*, 761.
17. Freeman, K. S.; Beck Tan, N. C.; Trevino, S. F.; Kline, S.; McGown, L. B.; Kiserow, D. J. *Langmuir* **2001**, *17*, 3912.
18. Laia César, A. T.; Pilar, L. C.; Costa Silvia, M. B.; d'Oliveira, J.; Martinho, J. M. G. *Langmuir* **1998**, *14*, 3531.
19. Chattopadhyay, D.; Mandal, B. M. *Langmuir* **1996**, *12*, 1585.
20. Simmons, B.; Agarwal, V.; McPherson, G.; John, V.; Bose, A. *Langmuir* **2002**, *18*, 8345.